

## Design and Biological Evaluation of Linear and Cyclic Phosphopeptide Ligands of the N-Terminal SH2 Domain of Protein Tyrosine Phosphatase SHP-1

Diana Imhof,\*<sup>†</sup> Karin Wieligmann,<sup>‡</sup> Kornelia Hampel,<sup>†</sup> Doreen Nothmann,<sup>†</sup> Mohammad S. Zoda,<sup>†</sup> Dirk Schmidt-Arras,<sup>§</sup> Martin Zacharias,<sup>||</sup> Frank D. Böhmer,<sup>§</sup> and Siegmund Reissmann<sup>†</sup>

*Institute of Biochemistry and Biophysics, Biological and Pharmaceutical Faculty, Friedrich-Schiller-University, Philosophenweg 12, 07743 Jena, Germany, Institute of Molecular Biotechnology, Theoretical Biophysics, Beutenbergstr. 11, 07745 Jena, Germany, Institute of Molecular Cell Biology, Medical Faculty, Friedrich-Schiller-University, Drackendorfer Str. 1, 07747 Jena, Germany, and School of Engineering and Science, International University Bremen, Campus Ring 8, 28759 Bremen, Germany*

Received October 22, 2004

In an effort to gain further insight into the conformational and topographical requirements for recognition by the N-terminal SH2 domain of protein tyrosine phosphatase SHP-1, we synthesized a series of linear and cyclic peptides derived from the sequence surrounding phosphotyrosine 2267 in the receptor tyrosine kinase Ros (EGLNpYMVL). A molecular modeling approach was used to suggest peptide modifications sterically compatible with the N-SH2-peptide binding groove and possibly enhanced binding affinities compared to the parent peptide. The potencies of the synthesized compounds were evaluated by assaying their ability to stimulate phosphatase activity as well as by their binding affinities to the GST-fused N-SH2 domain of SHP-1. In the series of linear peptides, structural modifications of Ros pY2267 in positions pY + 1 to pY + 3 by amino acid residues structurally related to Phe, for example *L-erythro/threo*-Abu( $\beta$ Ph) (**5a**, **5b**), yielded ligands with increased binding affinity. The incorporation of D-amino acid residues at pY + 1 and pY + 3 led to inactive peptides. The replacement of Phe in both pY + 1 and pY + 3 by Tic (1,2,3,4-tetrahydroisoquinoline-3-carboxylic acid) was also not tolerated due to steric hindrance. Cyclic peptides (**13**, **14**) that were linked via residues in positions pY – 1 (Lys) and pY + 2 (Asp/Glu) and contained a Gly residue in the bridging unit displayed much lower potencies for the stimulation of SHP-1 activity but increased binding affinities compared to Ros pY2267. They partially competed with Ros pY2267 in the activation assay. Such cyclic structures may serve as scaffolds for competitive SHP-1 inhibitor design targeting N-SH2 domain–protein interactions that block SHP-1 activation.

### Introduction

The reversible phosphorylation of proteins on tyrosine residues, as catalyzed by protein tyrosine kinases and phosphatases, is a principal mechanism by which eukaryotic cells respond to external stimuli.<sup>1</sup> Phosphorylated tyrosine residues, for example, on transmembrane receptors, form docking sites for proteins containing modular domains, such as Src homology 2 (SH2) or phosphotyrosine-binding (PTB) domains.<sup>2</sup> These domains provide phosphorylation- and sequence-specific interactions leading to the assembly of multisubunit complexes on receptors and subsequently to the initiation of intracellular signaling cascades. Due to its potential for signal transduction therapy, the development of strategies for the prevention of binding between phosphorylated activated receptors and SH2 domain containing interaction partners has become an attractive research field in medicinal chemistry.<sup>3,4</sup>

The cytoplasmic protein tyrosine phosphatase SHP-1 contains two SH2 domains amino-terminal to the phos-

phatase (PTP) domain and a short carboxy-terminal tail. SHP-1, expressed in hematopoietic and to a lesser extent in epithelial cells, has been recognized as a negative regulator of various immune cell functions, including antigen stimulation of B- and T-cells as well as neutrophil activity.<sup>5,6</sup> In osteoclasts, SHP-1 controls proliferation by negative regulation of CSF-1 receptor signaling.<sup>7</sup> Reduced levels of SHP-1 have been observed in different types of leukemia, which may indicate a role of SHP-1 deficiency in the process of carcinogenesis.<sup>8,9</sup> On the other hand, elevated expression of SHP-1 in human breast cancer led to the speculation that SHP-1 may play a positive role for proliferation of these cells.<sup>10</sup> Thus, effectors of SHP-1 activity may potentially be useful for modulation of immune cell function, bone resorption, or pathological cell proliferation.

Structural characterization of SHP-1 revealed that the N-terminal SH2 domain is primarily important for the catalytic activity of SHP-1. In the inactive state, the N-terminal SH2 domain blocks the catalytic domain. Binding of a phosphotyrosine (pTyr, pY) containing ligand leads to a conformational change within the N-SH2 domain upon which the PTP domain is released and thus accessible for substrate molecules.<sup>11,12</sup> Investigations on the recognition requirements of the SHP-1 N-SH2 domain revealed that the most critical interactions for high-affinity binding of phosphopeptide ligands

\* Corresponding author. Phone: +49 3641 949368. Fax: +49 3641 949352. E-mail: b4imidi@uni-jena.de.

<sup>†</sup> Institute of Biochemistry and Biophysics, Biological and Pharmaceutical Faculty, Friedrich-Schiller-University.

<sup>‡</sup> Institute of Molecular Biotechnology, Theoretical Biophysics.

<sup>§</sup> Institute of Molecular Cell Biology, Medical Faculty, Friedrich-Schiller-University.

<sup>||</sup> International University Bremen.

are binding in the pY and pY + 3 pockets, but also within the region occupied by the pY - 2 residue.<sup>13</sup> However, the conformational change that triggers the release from the entrance of the phosphatase domain and in turn induces phosphatase activation involves segments that are in contact with peptide residues distal to pY (C-terminal residues).<sup>11,12</sup> Previously, a combinatorial phosphopeptide library was used to determine the minimal sequence recognized by the N- and the C-terminal SH2 domain of SHP-1, respectively.<sup>14</sup> This study revealed that the SHP-1 N-SH2 domain selects for two consensus sequences, with a preference for LXpY(M/F)X(F/M) (X = any amino acid, M = Nle). Within this sequence, leucine was the most frequently occurring amino acid in position pY - 2. In position pY + 1, a norleucine residue that due to synthetic considerations has been introduced as an isostere for methionine was the most preferred amino acid, followed by phenylalanine. In contrast, a preference for phenylalanine prior to norleucine was found in position pY + 3. These data were consistent with the sequences of the majority of previously identified SHP-1 binding sites.

Recently, SHP-1 has been reported to bind to the activated epithelial receptor tyrosine kinase Ros by association of its N-terminal SH2 domain to Ros pY2267.<sup>15</sup> A comparison of the efficiency of Ros pY2267-N-SH2 domain binding to phosphorylated sequences derived from known interaction partners of SHP-1, such as EpoR pY429, Fc $\gamma$ RIIB1 pY309 and PILR $\alpha$  pY269, revealed that the Ros sequence displays a high-affinity ligand for the SHP-1 N-SH2 domain.<sup>16</sup> The sequence surrounding Ros pY2267 (LNpYMVL) is obviously in agreement with the minimal peptide sequence recognized by the N-SH2 domain of SHP-1 as determined by screening of the phosphopeptide library.<sup>14</sup>

To further characterize the conformational and topographical preferences of the N-terminal SH2 domain of SHP-1 for its phosphopeptide ligands we have selected and synthesized a series of peptides using the Ros pY2267 sequence as lead structure. Prior to peptide synthesis, computational tools have been used to pre-select structures on the basis of docking of a ligand into the protein domain binding site. One strategy to develop peptide ligands with high affinity and specificity for a particular binding site involves conformational constraining of a given sequence with the aim to restrict the peptide flexibility and to stabilize the biologically active conformation. Therefore, the flexibility of part of our linear peptides has been reduced by the introduction of nonproteinogenic and restricted amino acids. The structural flexibility of peptides can also be reduced by means of cyclization. Thus, we also incorporated cyclic structures in our series of N-SH2 ligands in order to obtain better conformational integrity. The peptides have been tested for their ability to stimulate SHP-1 activity, and binding affinities were determined by surface plasmon resonance. We obtained two types of ligands: High-affinity linear peptides that bind to the N-SH2 domain and stimulate SHP-1 activity better than the natural ligand and cyclic ligands that bind with high affinity but only weakly activate SHP-1. These new ligands allow us to separate binding and activation of SHP-1 and may form the basis for the design of antagonists that block the peptide binding site on the

**Table 1.** Synthesized Peptide Structures

no.	sequence <sup>a</sup>
class I <sup>b</sup>	Leu-Xxx-pTyr-Nle/Phe-Xxx-Phe/Nle <sup>c</sup>
Ros pY2267	H-Glu-Gly-Leu-Asn-pTyr-Met-Val-Leu-NH <sub>2</sub>
1	H-Glu-Gly-Leu-Asn-pTyr-Phe-Val-Leu-NH <sub>2</sub>
2	H-Glu-Gly-Leu-Asn-pTyr-Met-Val-Phe-NH <sub>2</sub>
3	H-Glu-Gly-Leu-Asn-pTyr-Hfe-Val-Leu-NH <sub>2</sub>
4	H-Glu-Gly-Leu-Asn-pTyr-Met-Val-Hfe-NH <sub>2</sub>
5	H-Glu-Gly-Leu-Asn-pTyr-Abu( $\beta$ Ph)-Val-Leu-NH <sub>2</sub>
6	H-Glu-Gly-Leu-Asn-pTyr-Met-Val-Abu( $\beta$ Ph)-NH <sub>2</sub>
7	H-Glu-Gly-Leu-Asn-pTyr-Ser( $\beta$ Ph)-Val-Leu-NH <sub>2</sub>
8	H-Glu-Gly-Leu-Asn-pTyr-Met-Val-Ser( $\beta$ Ph)-NH <sub>2</sub>
9	H-Glu-Gly-Leu-Asn-pTyr-Nle-Val-Phe-NH <sub>2</sub>
10	H-Glu-Gly-Leu-Asn-pTyr-Phe-Val-Phe-NH <sub>2</sub>
11	H-Glu-Gly-Leu-Asn-pTyr-Met-Tyr-Phe-NH <sub>2</sub>
12	H-Glu-Gly-Leu-Asn-pTyr-Tic-Ile-Tic-NH <sub>2</sub>
13	H-Glu-Gly-Leu-Lys-pTyr-Met-Asp-Leu-NH <sub>2</sub> $\text{OC}-\text{CH}_2-\text{NH}$
14	H-Glu-Gly-Leu-Lys-pTyr-Met-Glu-Leu-NH <sub>2</sub> $\text{OC}-\text{CH}_2-\text{NH}$
15	H-Glu-Gly-Leu-Lys-pTyr-Met-Glu-Leu-NH <sub>2</sub>

<sup>a</sup> Single letter amino acid designation was avoided due to modifications by non-natural amino acids. Xxx indicates a position in which all amino acids can be included. <sup>b</sup> Class I consensus sequence according to the literature.<sup>14</sup> <sup>c</sup> Nle has been used as an isostere for Met.<sup>14</sup>

N-SH2 domain of SHP-1 without activation of the phosphatase.

## Results and Discussion

**Selection of Peptide Structures.** In contrast to other SH2 domains,<sup>3,4</sup> the majority of the ligands for the SHP-1 N-SH2 domain described to date represents linear phosphopeptides derived from interacting proteins and corresponds to the binding motif obtained by screening of a phosphopeptide library.<sup>14</sup> These peptides are rather flexible molecules. To gain further insight into the recognition features of the SHP-1 N-SH2 domain, we focused our interest on the generation of conformationally restricted structures derived from the sequence Glu-Gly-Leu-Asn-pTyr-Met-Val-Leu (EGLNpYMVL) of the receptor tyrosine kinase Ros (Table 1). However, the series of our ligands presented here not only includes constrained peptides (**12–15**) but also analogues containing the most preferred amino acids in the relevant positions according to the class I consensus sequence LXpYM/FXF/M (**1, 2, 9, 10, 11**).<sup>14</sup> The amino acid Leu in position pY - 2 is known as one effective specificity determinant for recognition by the N-SH2 domain of SHP-1. Since this residue is already contained in the native sequence of Ros pY2267, we kept it in all of our synthetic analogues. According to the consensus sequence, residues at pY - 1 and pY + 2 play only minor roles for recognition by the N-SH2 domain. Therefore, the residues Asn and Val that naturally occur in the Ros sequence were retained in most analogues,

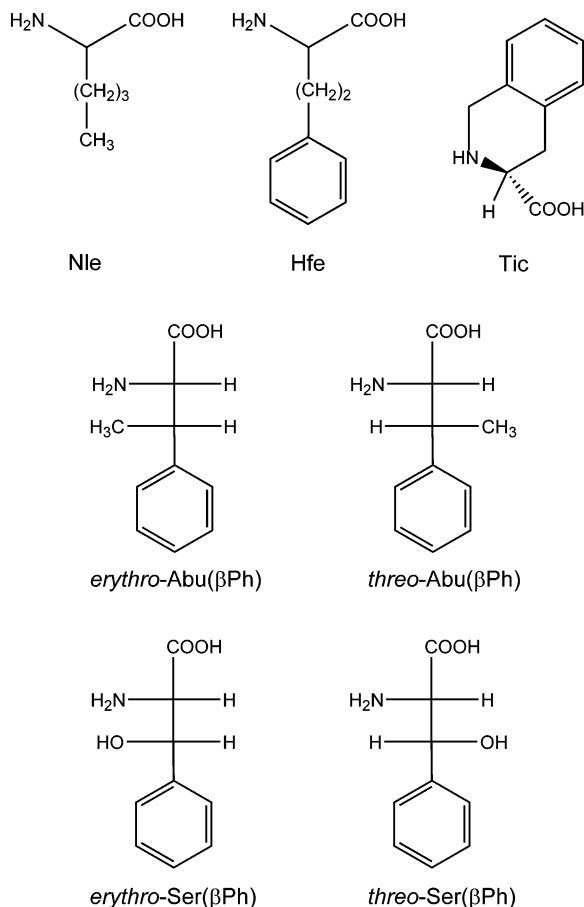


**Figure 1.** Structural formulas of the used hydrophobic non-natural amino acid residues.

too. Furthermore, we have produced the peptides as C-terminal carboxyamides, since the carboxyl group does not make significant contacts with the protein. Our approach may be regarded as step by step elucidation of the structural limitations for modifications of the SHP-1 N-SH2 domain binding motif.

The studied linear structures contain amino acid substitutions in positions pY + 1, pY + 2, and pY + 3, respectively, compared to the parent peptide Ros pY2267 (Table 1). Since the N-SH2 domain prefers hydrophobic and, in particular, aromatic amino acids in positions pY + 1 and pY + 3 we were searching for suitable substitutions mimicking these properties. In early studies on analogues of the peptide hormone bradykinin, the diastereomeric threo- and erythro-forms of  $\beta$ -phenylserine (Ser( $\beta$ Ph)) and  $\alpha$ -amino- $\beta$ -phenylbutyric acid (Abu( $\beta$ Ph)) have successfully been introduced in place of phenylalanine (Figure 1).<sup>23–25</sup> Both phenylalanine substitutions are considered to represent structures in which the phenyl ring is configurationally stabilized through the C $\beta$ -substituent. Besides Abu( $\beta$ Ph) (**5**, **6**) and Ser( $\beta$ Ph) (**7**, **8**), also homophenylalanine (Hfe) that only differs from phenylalanine in one further methylene group between the C $\alpha$ -atom and the aromatic ring<sup>26</sup> was introduced in our studies (**3**, **4**) (Figure 1).

As a result of investigations in which conformational and topographical constraints have been used for the design of biologically active peptides,<sup>27,28</sup> an array of amino acids with complementary conformational properties compared to the natural precursor is available today.<sup>29</sup> The concept of topographical design is aimed

at a particular three-dimensional arrangement of the peptide side chains through appropriately constraining, biasing, or fixing the side chain conformers. As an example, phenylalanine side chain conformations can be constrained by the use of 1,2,3,4-tetrahydroisoquinoline-3-carboxylic acid (Tic) (Figure 1).<sup>27,28,30,31</sup> Thus, we chose to incorporate it in our investigations (peptide **12**). We also generated cyclic structures (**13–15**) that have a reduced flexibility compared to the linear ligands aiming at a stabilization of the conformation when bound to the protein domain. The selection of these structures was according to the docking results of the molecular modeling approach and is described in the section below. Because of the hydrophobic nature of the analogues, all peptides were prolonged N-terminally by two amino acids (glutamic acid and glycine) naturally occurring in the Ros sequence to ensure solubility for biological testing.

**In Silico Screening.** The recent determination of the crystal structure of SHP-1 and the available structural data of the homologous SHP-2 as well as its N-SH2 domain in the peptide complexed and free form<sup>12,21,22,32</sup> have supported our screening efforts. No crystal structure of the SHP-1 N-SH2 domain in complex with a high-affinity peptide ligand is hitherto available. However, the N-SH2 domains of SHP-1 and SHP-2 share >60% sequence identity that allows us to build an accurate homology model of the N-SH2 domain of SHP-1 based on the crystal structure of the SHP-2 N-SH2-domain in complex with the natural ligand PDGFR pY740 (PDB code 1AYC). A homology model was generated by replacing the residues of SHP-2 that are involved in ligand binding with the corresponding ones of SHP-1. The binding orientation of the natural ligand observed in the crystal structure of SHP-2 is conserved for all compounds included in this study. It is important to note that some of the residues that were replaced in the SHP-2 N-SH2 template structure by the corresponding residues of SHP-1 contact the pY residue of the bound peptide (e.g. Lys36). However, none of the substitutions directly contact the residues pY + 1 and pY + 3 of the bound peptide that are at the focus of the current investigation.

In Figure 2 the docking of the native ligand Ros pY2267 into the N-terminal SH2 domain of SHP-1 is shown. The peptide adopts an extended conformation with intensive contacts of residues pY – 2, pY, pY + 1, and pY + 3 with the corresponding binding pockets that is in full agreement with the specificity determinants suggested in the literature.<sup>14</sup> In the pY – 2 pocket, main contacts are between the Leu residue in the peptide ligand with Gly13 and Leu14 of the SH2 domain. The positively charged pY pocket is formed by Arg32, Lys36, His53, and Arg55. The binding pocket occupying residues pY + 1 and pY + 3 of the peptide ligand is a hydrophobic depression formed by Ile54, Leu88, Ile 96, and Thr52 (pY + 1) as well as Tyr66, Ile54 and Arg55 (pY + 3).

The modified peptides (Table 1) were docked into the N-SH2 domain and energy minimized. The ranking of the peptide–SH2 complexes is based on the sterical and electrostatic fit between ligand and SH2 domain, and the interaction energies were determined relative to the parent peptide Ros pY2267 (Table 2). The main purpose





**Table 2.** Ranking of Interaction Energies, SHP-1 Activity, and Binding Assay Results of the Synthesized Peptide Analogues

no.	isomer	energy (kcal/mol) <sup>a</sup>	EC <sub>50</sub> ( $\mu$ M)	K <sub>d</sub> ( $\mu$ M) <sup>b</sup>
Ros pY2267		0	160	1.44 $\pm$ 0.45
1		-3	70	0.69 $\pm$ 0.21
2		-9	140	1.00 $\pm$ 0.01
3		-2	140	0.90 $\pm$ 0.30
4		-6	75	0.27 $\pm$ 0.10
5a	<i>L-threo</i> -Abu( $\beta$ Ph)	-6	50	0.24 $\pm$ 0.13
5b	<i>L-erythro</i> -Abu( $\beta$ Ph)	-7	220	0.16 $\pm$ 0.11
5c	<i>D-threo</i> -Abu( $\beta$ Ph)	<i>c</i>	na	nb
5d	<i>D-erythro</i> -Abu( $\beta$ Ph)		na	nb
6a	<i>L-threo/erythro</i> -Abu( $\beta$ Ph)	-8/-12	70-80	0.25 $\pm$ 0.01
6b	<i>D-threo/erythro</i> -Abu( $\beta$ Ph)		180	nb
7a	<i>L-threo</i> -Ser( $\beta$ Ph)	-4	220	1.08 $\pm$ 0.10
7b	<i>D-threo</i> -Ser( $\beta$ Ph)		na	nb
8a	<i>L-threo</i> -Ser( $\beta$ Ph)	-9	85	0.29 $\pm$ 0.02
8b	<i>D-threo</i> -Ser( $\beta$ Ph)		na	nb
9		-10	50-60	0.23 $\pm$ 0.10
10		-12	50	0.12 $\pm$ 0.02
11		-8	150	0.53 $\pm$ 0.11
12		+1.9	na	nb
13		-4	na	0.11 $\pm$ 0.01
14		-2	na	0.21 $\pm$ 0.07
15		+12	na	nb

<sup>a</sup> Ranking of the calculated interaction energy relative to Ros pY2267 (0 kcal/mol). <sup>b</sup> Peptides for SPR measurements were prolonged N-terminally by biotin-Ado. <sup>c</sup> For D-amino acid containing peptides, no values are given due to unfavorable conformation leading to interruption of necessary contacts within binding pockets pY + 1 and pY + 3, respectively; na, not active, where maximal activity was  $\leq 0.4$  relative to Ros pY2267; nb, no binding, where maximum change in RU was  $< 20$ .

of each diastereomer will be the focus of a subsequent paper.<sup>17</sup> The stereochemistry was assigned as shown in Table 2. With respect to their potency to stimulate SHP-1 activity, we found that the presence of *D-threo*- or *D-erythro*-Abu( $\beta$ Ph) in analogues **5c** and **5d** was detrimental to activity, since both peptides were inactive. A convincing explanation for this result might be the fact that peptides containing a D-amino acid residue have a different conformation compared to the L-configured counterparts when bound to the protein domain. This assumption could be confirmed by the molecular modeling studies which showed that the aromatic ring in both D-Abu( $\beta$ Ph)-containing peptides (**5c**, **5d**) is directed toward the surface of the SH2 domain and does not bind into the pY + 1 pocket. In contrast, the peptides containing *L-threo*-Abu( $\beta$ Ph) (**5a**) and *L-erythro*-Abu( $\beta$ Ph) (**5b**) showed better or similar activities compared to the reference peptide, but in the case of peptide **5a**, SHP-1 activity decreased at peptide concentrations  $> 200 \mu$ M (Figure 3). Maximum activity for this peptide is reached at  $180 \mu$ M, higher concentrations obviously result in inhibition, probably due to competition with the substrate at the enzymes active site. Analysis of the conformations of **5a** and **5b** when docked into the SH2 domain revealed that for the *erythro*-form of L-Abu( $\beta$ Ph) (**5b**), the aromatic ring is slightly rotated (about  $45^\circ$ ) compared to the position of the Phe side chain in analogue **1**, whereas in the case of the *L-threo*-Abu( $\beta$ Ph)-containing peptide **5a** it is about  $90^\circ$ . The methyl group on the C $^\beta$ -atom of the *L-threo*-Abu( $\beta$ Ph) side chain shows additional contacts to Thr52, Ile96, and Ile54 and has a different orientation compared to the *L-erythro*-isomer, where this methyl group can interact with the Leu8 side chain of the ligand itself. The *erythro/threo* configuration of Abu( $\beta$ Ph) in these peptides caused no significant difference in the interaction energies obtained from the molecular modeling approach (Table 2). Although the value for half-maximal activation of compound **5b** is higher (EC<sub>50</sub>  $\sim 220 \mu$ M)

than that obtained for Ros pY2267, at  $500 \mu$ M peptide concentration, SHP-1 activity is exceeding that of the parent peptide, suggesting that **5b** has a lesser capacity to compete with pNPP substrate than Ros pY2267.

It was thought that Ser( $\beta$ Ph) at pY + 1 as occurring in peptide **7** would perform a similar role as Abu( $\beta$ Ph) in the same position, since the only structural difference is a hydroxy group on the C $^\beta$ -atom instead of the methyl group as in Abu( $\beta$ Ph). Because of the easier synthetic accessibility of the *threo*-configured Ser( $\beta$ Ph) compared to the *erythro*-form and considering that the modeling studies revealed no significant difference in the interaction energies between both isomers, we decided to only incorporate D/L-*threo*-Ser( $\beta$ Ph) in peptides **7** and **8**.<sup>17,23,25</sup> As shown in Figure 3, analogue **7a** (*L-threo*) stimulated SHP-1 activity with half-maximal activation reached at  $\sim 220 \mu$ M, whereas the *D-threo* analogue **7b** was inactive (Figure 3, Table 2). The lower activity of the *L-threo*-Ser( $\beta$ Ph)-containing analogue **7a** compared to the reference peptide cannot be explained by the docking result, since the position and orientation of the aromatic rings of the pY + 1 residue in analogues **1** and **7a** are congruent and the hydroxy group shows an additional interaction with Glu90 of the N-SH2 domain that seemed advantageous for binding affinity.

Abu( $\beta$ Ph) and Ser( $\beta$ Ph) have also been incorporated in position pY + 3 (**6** and **8**) instead of Phe (**2**). In contrast to peptide **5**, we could only separate two peaks in the HPLC analysis of compound **6**, which according to the racemization studies represent a mixture of *L-threo/erythro*-Abu( $\beta$ Ph) (**6a**) and *D-threo/erythro*-Abu( $\beta$ Ph) (**6b**) (Table 2).<sup>17</sup> For the first fraction (**6a**), an EC<sub>50</sub> of  $\sim 70-80 \mu$ M has been determined, whereas fraction **6b** reached half-maximal activation at  $\sim 180 \mu$ M (Figure 3). The same was found for the two diastereomers of the D/L-*threo*-Ser( $\beta$ Ph)-containing peptide **8**. The peptide with the *L-threo* form (**8a**) also stimulated SHP-1 activity better than the reference peptide (EC<sub>50</sub>  $\sim 85 \mu$ M), whereas the *D-threo*-Ser( $\beta$ Ph) analogue **8b** was

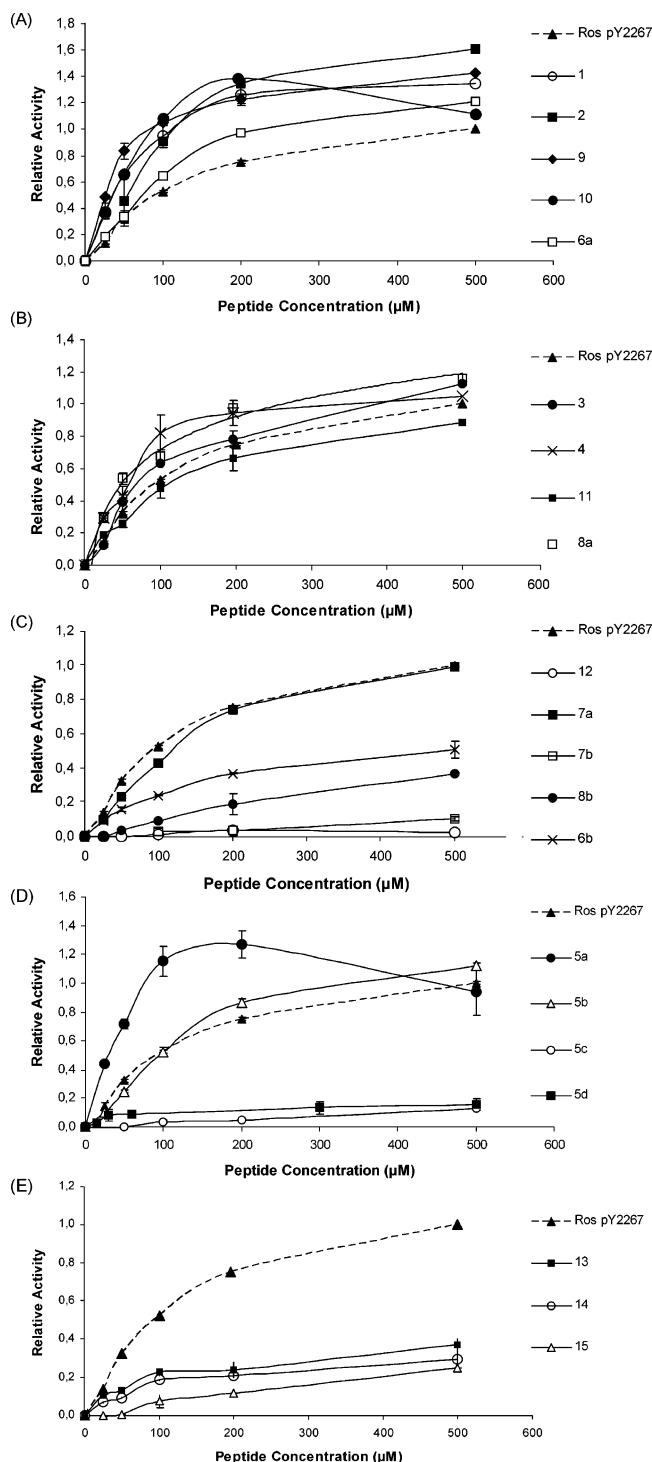


**Figure 3.** Activation of SHP-1 by N-SH2 domain ligands. SHP-1 activity relative to that of Ros pY2267 (1.0 at 500  $\mu\text{M}$ ) is plotted against the peptide concentration. The dashed line in all figures represents the data obtained for the parent Ros pY2267. (A) peptides with increased SHP-1 activity; (B) peptides stimulating SHP-1 activity comparable to Ros pY2267; (C) peptides with decreased or without SHP-1 activity; (D) fractions a–d of peptide 5 containing Abu( $\beta\text{Ph}$ ); (E) activation of SHP-1 by cyclic peptides.

much less active than the parent Ros pY2267 (Figure 3). Thus, the D-configuration again reduced the capacity for the stimulation of SHP-1 activity. However, the effect is not as strong as in peptides **5c**, **5d**, and **7b**, which contained either D-Abu( $\beta\text{Ph}$ ) or D-Ser( $\beta\text{Ph}$ ), at pY + 1. This may be due to the position of the D-amino acid

residue, i.e., the negative effect is not as significant in the C-terminus (pY + 3) of the peptides as in the core region (pY + 1). The amino acid at pY + 3 occupies a hydrophobic pocket mainly made up of Tyr66, Ile54, and Arg55. Considering the conformational shape of analogues **2**, **6a**, and **8a** when docked into the N-SH2 domain, it can be seen that the aromatic ring in the side chains of Phe, Abu( $\beta\text{Ph}$ ), and Ser( $\beta\text{Ph}$ ) has exactly the same position and orientation and the interaction energies are in the same range. The improved activities of peptide **6a** (Abu( $\beta\text{Ph}$ )) or **8a** (Ser( $\beta\text{Ph}$ )) may therefore be explained by a stabilization of the phenyl ring through the additional methyl group (**6a**) and hydroxy group (**8a**), respectively, that positively influenced the binding behavior compared to analogue **2** (Phe) with a more flexible phenyl ring.

Peptides **9** (Nle6), **10** (Phe6, Phe8), and **11** (Tyr7, Phe8) were prepared in order to find out about the amino acid preferences of pY + 1 to pY + 3 within the lead structure Ros pY2267. Here, we used those residues that were suggested by Beebe et al.<sup>14</sup> Due to the fact that the native peptide contained Met at pY + 1, we also checked the influence of its replacement by Nle (**9**) on the activity of the parent peptide. This amino acid has also been incorporated for Met in the combinatorial peptide library.<sup>14</sup> We intended to find out differences between the Met substitutions Phe, Hfe, Abu( $\beta\text{Ph}$ ), Ser( $\beta\text{Ph}$ ), and Nle to further characterize the structural requirements for a residue occupying the pY + 1 pocket. Furthermore, we tested the effectiveness of combining two substitutions with the peptides containing Phe at positions 6 and 8 (**10**) as well as Tyr at 7 and Phe at 8 (**11**), respectively. Peptides **9** and **10** belong to the most active compounds in the reported series, showing half-maximal activation at  $\sim 50 \mu\text{M}$ . However, for peptide **10**, the activity decreased at peptide concentrations  $> 200 \mu\text{M}$ , as was already observed for peptide **5a**. Here, the maximal activity is reached at 190  $\mu\text{M}$ , and higher concentrations of peptide again result in inhibition of SHP-1. Comparing compounds **9** and **10** with the Ros pY2267 ligand, we can conclude that replacing both Met6 and Leu8 by Nle/Phe6 and Phe8 is preferable with respect to phosphatase activity. It should also be noted that according to the modeling results, the occurrence of two aromatic side chains is favorable. The Phe residues in peptide **10** are close together and hydrophobic interactions of the two aromatic rings within the pocket for pY + 1 and pY + 3 can be observed. Considering the peptides selected by the phosphopeptide library,<sup>14</sup> it can be seen that the sequence of compound **10** (LNpYFVF) is comparable to the selected peptide LNpYFAF with respect to specificity determinants.

Compound **11** represents a sequence that contains substitutions at pY + 2 and pY + 3. Its C-terminal hexapeptide sequence was selected by screening of the phosphopeptide library.<sup>14</sup> We introduced it in our study for reasons of comparison, in particular, to evaluate its potency versus the most active peptides obtained in this study. We found that it is not as potent as peptides **1**, **2**, **9**, and **10** but comparable to the reference peptide Ros pY2267. A possible explanation for this finding is the fact that the Tyr side chain at pY + 2 that is not occupied by a distinct pocket on the SH2-domain is too



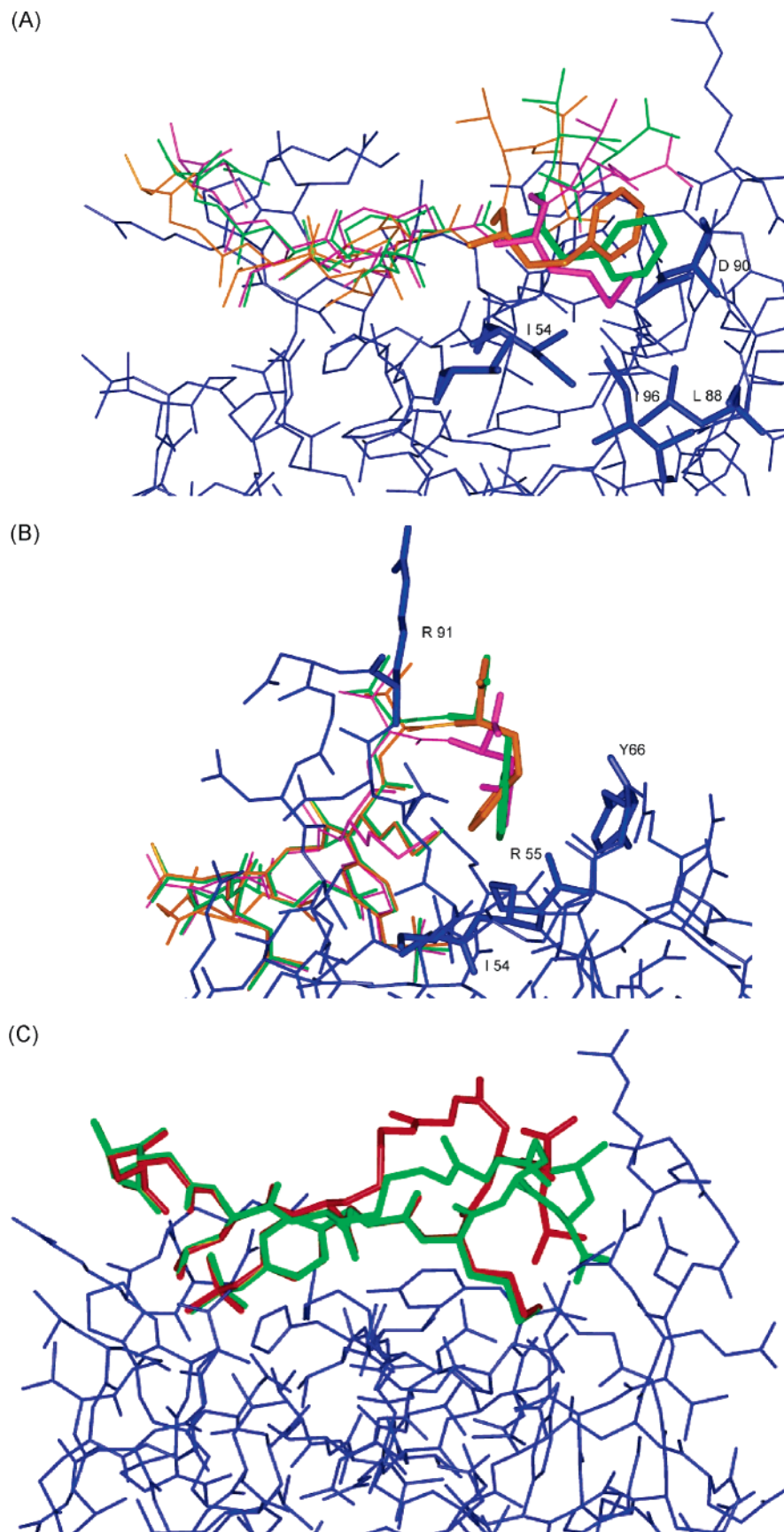


**Figure 4.** Interactions of individual residues of different peptides with the N-SH2 domain of SHP-1 (blue). (A) superimposition of phosphopeptides Ros pY2267 (pink), **1** (green), and **3** (orange) with residues at pY + 1 highlighted; (B) superimposition of Ros pY2267 (pink), **2** (green), and **4** (orange) with residues at pY + 3 highlighted; (C) docking of cyclic compounds **13** (red) and **14** (green) into SHP-1 N-SH2 domain (blue).

long and therefore more exposed to the solvent, e.g., compared to the shorter side chains of Ala and Val.

Compound **12** contains Tic instead of Phe at both pY + 1 and pY + 3. In agreement with the modeling predictions, the peptide was found to be inactive with respect to stimulation of SHP-1 activity (Figure 3, Table 2). The Tic residue as imino acid leads to a more turnlike-shaped backbone in the C-terminal region, and additionally, two Tic residues are too large to be buried in the pocket for pY + 1 and pY + 3 on the SH2 domain.

In general, it can be stated that the linear structures that stimulate the phosphatase activity of SHP-1 were consistent with the theoretical predictions. In contrast, the cyclic peptides behaved differently. Compounds **13** and **14** were designed with the intent to reduce the conformational flexibility of the linear lead structure. These peptides only differ in position pY + 2, where Asp (**13**) and Glu (**14**) have been introduced. According to the modeling studies, it is favorable to incorporate a glycine residue in the bridging unit. To test this assumption, peptide **15** was additionally synthesized and biologically evaluated. Surprisingly, all cyclic structures displayed much lower potencies in stimulating SHP-1 phosphatase activity than Ros pY2267 (Figure 3). For these peptides, no EC<sub>50</sub> values were given, since phosphatase activity at 500  $\mu$ M was only <0.4 compared to 1.0 for Ros pY2267 (Table 2).

**Interaction Analysis.** The evaluation of potential N-SH2 domain ligands by the SHP-1 activation assay is limited in that it gives only semiquantitative data and leaves ligands undetected that might bind to the SH2 domain without activating the enzyme. Therefore, the  $K_d$  values for the interaction of the immobilized biotinylated phosphopeptides with the GST-N-SH2 domain of SHP-1 were determined using SPR. We incorporated 8-amino-3,6-dioxaoctanoic acid (Ado) as a spacer between biotin and the N-terminus of the peptides to improve the accessibility of the immobilized peptides on the streptavidin-coated sensorchips and to increase the solubility of the hydrophobic peptides. In Table 2 the data for the measured interactions are summarized. A typical SPR sensogram exemplified by the peptide **6a** is shown in Figure 5.

The  $K_d$  value for Ros pY2267 (1.44  $\mu$ M) is in close agreement with the literature data reported for similar peptides that were selected from the phosphopeptide library.<sup>14</sup> It should be noted that the sequence analyzed here is significantly shorter than a previously described pY2267 Ros peptide that had a higher affinity.<sup>16</sup> The finding that compounds **5c**, **5d**, **6b**, **7b**, and **8b** containing a D-amino acid residue were less active or inactive in stimulating SHP-1 activity could be confirmed with the SPR measurements. All these peptides displayed binding affinities lower by 2 orders of magnitude or even lower compared to that of the parent peptide Ros pY2267. Also, a lack of detectable binding in the SPR studies of peptides **12** and **15** was consistent with their low capacity to activate SHP-1. Obviously, the bulky Tic moieties in compound **12** sterically impede optimal formation of the SH2 domain-peptide complex. Whereas, for the cyclic peptide **15** we suggest that the strained ring formed upon direct linkage of Lys (pY - 1) and Glu (pY + 2) prevents the peptide from adopting the extended backbone conformation required for associa-

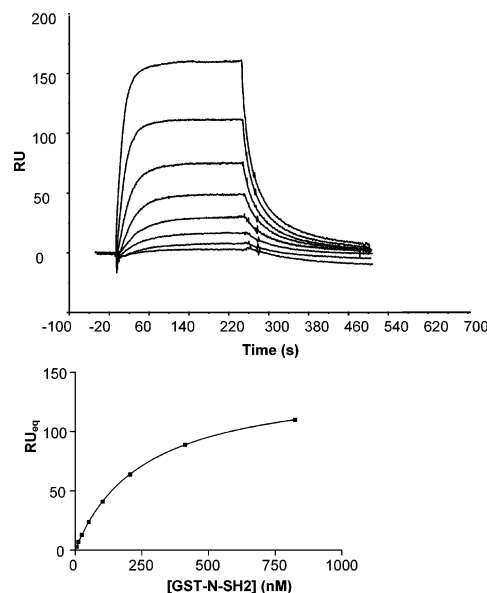


**Figure 5.** Sensogram for the binding of the GST-N-SH2 domain of SHP-1 to immobilized phosphopeptide **6a** (A) with concentrations of GST-N-SH2 (SHP-1) ranging from 0 to 750 nM. (B) Resonance units under equilibrium conditions plotted against the GST-N-SH2 domain concentration.

tion with the N-SH2 domain of SHP-1. Also, the differences in the binding affinities within the series of linear peptides were in most cases consistent with the data obtained from the phosphatase assay. For peptides **1** and **2**, the  $K_d$  values were slightly better than that of the lead peptide Ros pY2267 with a  $\sim$ 2-fold higher affinity for compound **1** (Table 2). These peptides also showed different results in the activation assay where peptide **1** was more potent than peptide **2** and the native peptide. In contrast to the Phe-containing peptides, we obtained values of 0.90 and 0.27  $\mu$ M for compounds **3** (Hfe6) and **4** (Hfe8), respectively. These values are consistent with the molecular modeling results as well as the values from the phosphatase assay. Interestingly, compound **4** exhibits a nearly 5-fold higher affinity to the N-SH2 domain than the parent peptide Ros pY2267 and a  $\sim$ 3-fold higher affinity than peptide **3**. This again suggests that the longer side chain of Hfe versus Phe is preferred at pY + 3.

The affinities of compounds **5a** (*L-threo*-Abu( $\beta$ Ph)6) and **5b** (*L-erythro*-Abu( $\beta$ Ph)6) (0.24 and 0.16  $\mu$ M) for the N-SH2 domain were among the highest reported in this series, comparable to the affinities displayed by the potent linear peptides **9** (0.23  $\mu$ M) and **10** (0.12  $\mu$ M). We therefore assume that the mentioned additional contacts of the C $^{\beta}$ -methyl group of *L-threo*-Abu( $\beta$ Ph) with Thr52 and Ile96 as well as of *L-erythro*-Abu( $\beta$ Ph) with the Leu8 side chain of the peptide positively contribute to the binding affinities.

In contrast to the high-affinity compounds **5a** and **5b**, peptide **7a** with *L-threo*-Ser( $\beta$ Ph) in position 6 displayed a  $K_d$  value of 1.08  $\mu$ M that is only slightly better than that of the lead peptide. These results led to the conclusion that a methyl group at the C $^{\beta}$ -atom is preferred over a hydroxy group due to favorable additional interactions with the protein domain. The Abu( $\beta$ Ph)8 containing analogue **6a** showed a  $\sim$ 6-fold higher affinity to the SH2 domain compared to Ros pY2267 (Figure 5, Table 2). This is in the range of the value



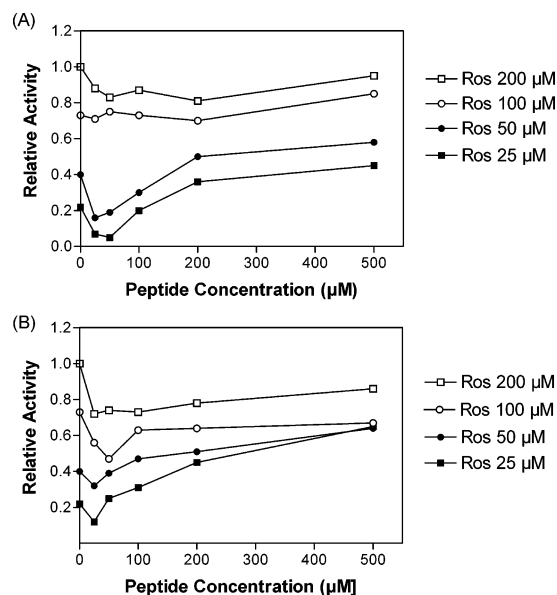


**Figure 6.** Activation of SHP-1 by Ros pY2267 in the presence of the cyclic peptides **13** (A) and **14** (B). The stimulated phosphatase activity was plotted against the concentration of cyclic peptide.

obtained for the Hfe8-containing peptide **4** and also peptide **8a** with *L*-threo-Ser( $\beta$ Ph)**8**. These three compounds showed a similar behavior in the phosphatase assay. Compared to the potent and high-affinity peptides **9** and **10**, we found a  $K_d$  value of  $0.53 \mu\text{M}$  for compound **11** that is better than the value obtained for the native Ros pY2267, although in the phosphatase assay the results for both peptides were comparable (Figure 3, Table 2).

However, the most interesting results were obtained for the cyclic peptides. In contrast to their relatively low potency to stimulate SHP-1 activity, compounds **13** and **14** showed  $K_d$  values of  $0.11$  and  $0.21 \mu\text{M}$ , respectively, that are in the range of the active peptides **9** and **10**. If the peptides **13** and **14** bind with high affinity but still do not activate SHP-1, then they might compete with the natural ligand with respect to SHP-1 activation. Indeed, when the ability of Ros pY2267 to activate SHP-1 was tested in the presence of the cyclic peptides (**13**, **14**), a partial inhibition was observed (Figure 6). The effect is stronger for peptide **14** than for peptide **13**. This could be observed at  $100$  and  $200 \mu\text{M}$  Ros pY2267. At lower Ros pY2267 concentrations ( $25$  and  $50 \mu\text{M}$ ), the competition was also weakly detectable for low concentrations of cyclic peptides but not at higher concentrations. Presumably, the still existing weak activating effect of **13** and **14** dominated over the competition under these conditions.

## Conclusions

On the basis of the library-derived class I consensus sequence LXpYM/FFX/M (X = any amino acid, M = Nle) and the sequence of natural interaction partner Ros pY2267 (EGLNpYMVL), we designed and synthesized a series of linear and cyclic peptides for the SHP-1 N-SH2 domain guided by molecular modeling. The available information on the SH2 domains of SHP-1 and the homologous SHP-2 supported our search for high-affinity N-SH2 ligands which aimed at a deeper understanding the important regions of the interface and

identifying new structural features of the N-SH2 domain–ligand interaction. We mainly introduced residues at pY + 1 and pY + 3 mimicking Phe, such as Hfe, Abu( $\beta$ Ph), Ser( $\beta$ Ph), and Tic. As expected, linear peptides strongly related to the N-SH2 domain binding motif effectively stimulated phosphatase activity and bound to the GST-N-SH2 domain with high-affinity as determined by surface plasmon resonance. However, slight differences in the structural requirements for binding in the pY + 1 and pY + 3 pockets were observed. From the modeling efforts, it was evident that the pY + 1 and pY + 3 pockets formed by hydrophobic residues of the protein surface could tolerate hydrophobic amino acids in the relevant positions of the ligand. We thought that a longer side chain at position pY + 1 or pY + 3, such as the one of Hfe, might be able to better access this hydrophobic surface. However, we found that amino acids such as Phe (**1**), Nle (**9**), or *L*-Abu( $\beta$ Ph) (**5**) gave better biological results than the Hfe-containing peptide **3** when introduced at pY + 1, whereas at pY + 3 residues other than Phe (**2**), like Hfe (**4**), *L*-Abu( $\beta$ Ph) (**6**), and *L*-Ser( $\beta$ Ph) (**8**), were better with respect to the results of the biological assays. Also, the additional hydroxy group at the  $C^\beta$ -atom of *L*-Ser( $\beta$ Ph) in position pY + 1 of peptide **7** is not favorable over the other substitutions mentioned above. Interestingly, the hydrophobic and less flexible imino acid residue Tic incorporated at pY + 1 and pY + 3 within the conformationally restricted peptide **12** was predicted to be sterically unfavorable for binding to the protein domain. The prediction was confirmed experimentally by the lack of phosphatase activation and of binding affinity for compound **12** as compared with parent Ros pY2267. Besides, according to our results, it can be concluded that stereochemistry at positions pY + 1 and pY + 3 is important to maintain activity, since all analogues with D-residues in these positions were inactive or less active and did not associate with the N-SH2 domain with high-affinity.

Beside the linear structures, we are interested in conformationally restricted peptides in order to reduce the flexibility of the ligands and through this to enhance the biological effects. Regarding the N-SH2 domain–ligand association, specific interactions anchor the phosphopeptide in an extended conformation that allows the side chains of the C-terminal residues to reach specificity pockets on the protein. To avoid interference with the residues important for binding in these pockets, we generated peptides cyclized between pY – 1 (Lys) and pY + 2 (Asp, Glu). In addition, a ring size suitable to maintain the extended backbone had to be chosen. According to the theoretical predictions, this could be performed by introducing Gly in the bridging unit. A peptide lacking this Gly is unable to assume the extended conformation when it binds to the SHP-1 N-SH2 domain due to interruption of the necessary contacts at pY + 1 and pY + 3. The experimental data confirmed these observations, since peptide **15** did not bind to the SH2 domain and was also inactive with respect to stimulation of SHP-1 activity. The most surprising results, however, were obtained for the two cyclic compounds **13** and **14**. Both peptides displayed much lower activities than the native ligand Ros pY2267 in the phosphatase activation assay but show higher binding affinities. This led us to examine their ability

to inhibit SHP-1 activity in the presence of Ros pY2267. The competition experiment revealed that the cyclic peptides partially inhibit Ros pY2267-mediated SHP-1 activation.

Structural studies on SHP-1 and SHP-2<sup>11,12</sup> indicate that activation of the SHP-1 phosphatase requires not only high-affinity binding of a peptide to the N-SH2 domain but also triggering of a conformational change in the N-SH2 that in turn leads to a release of the N-SH2 domain from the entrance of the phosphatase domain. The conformational change requires SH2 domain-segments that are in contact with the C-terminal part of a bound peptide (e.g. residue pY + 3). A possible structural explanation for the inhibitory effect of the cyclic peptides is that the conformational restriction may enhance the binding affinity due to stabilization of the backbone conformation in the bound form but at the same time slightly distort the binding geometry of the pY + 1 and pY + 3 residues. This is also suggested by the modeling studies (Figure 4c). Despite the high binding affinity of these peptides, the imperfect binding geometry of the pY + 1 and pY + 3 residues is in turn insufficient to trigger the allosteric conformational change in the N-SH2 domain required for phosphatase activation. In contrast, linear peptides with bulky residues at pY + 1 and pY + 3 fill the binding cavities completely and efficiently trigger the conformational transition in the N-SH2 domain necessary for the dissociation of the phosphatase domain; hence, ligand binding leads to strong SHP-1 activation.

In summary, our results suggest several peptide modifications that lead to enhanced peptide binding to the N-SH2 domain of SHP-1. In addition, two classes of modifications were found that either lead to increased phosphatase activation compared to the parent Ros pY2267 peptide or to a partially competitive inhibition of phosphatase activation (cyclic peptides). This result may form the basis for the rational design of inhibitors for SHP-1 that interfere with N-SH2 domain–protein interaction and block of phosphatase activation.

## Materials and Methods

**Abbreviations:** Ado, 8-amino-3,6-dioxo-octanoic acid; GST, glutathione *S*-transferase; N-SH2, N-terminal Src homology 2 domain; PDGFR, platelet derived growth factor receptor; PTB, phosphotyrosine binding domain; pNPP, *p*-nitrophenyl phosphate; SPR, surface plasmon resonance.

**Materials.** All chemicals used were of reagent grade from Fluka (Sigma-Aldrich, Taufkirchen, Germany). Biomol green was obtained from Biomol GmbH (Hamburg, Germany). The proteins were purified using glutathione sepharose 4B (Amersham Biosciences, Freiburg, Germany) and eluted with a poly-prep column (Biorad, München, Germany) using reduced glutathione (Sigma-Aldrich, Taufkirchen, Germany). Protease Factor Xa was purchased from New England Biolabs (Frankfurt/Main, Germany). Streptavidin-coated chips were from Biacore International SA (Freiburg, Germany).

**Phosphopeptide Synthesis.** Solid-phase synthesis of the phosphopeptides is described in more detail elsewhere.<sup>17</sup> Biotinylation of the peptides has been carried out on the solid phase using PyBop (benzotriazol-1-yloxytrispyrrolidinophosphonium hexafluorophosphate) as coupling reagent. Release of biotinylated peptides from the polymer support with concomitant cleavage of side chain protecting groups has been achieved using 95% trifluoroacetic acid, 2.5% water, and 2.5% triisopropylsilane. The crude peptides were purified by semi-preparative reversed-phase HPLC (Shimadzu LC-8A, Duisburg, Germany) equipped with a C<sub>18</sub> column (Knauer Euro-

spher 100, Berlin, Germany) prior to use. Purity and identity of the peptides were established by analytical reversed-phase HPLC (Shimadzu LC-10AT, Duisburg, Germany), MALDI mass spectrometry (Perseptive Biosystems, Weiterstadt, Germany), and amino acid analysis (Eppendorf-Biotronik, Hamburg, Germany). The peptide concentrations were determined by quantitative amino acid analysis after complete hydrolysis (6 N HCl, 110 °C, 24 h) of an aliquot of the peptide solutions and by the malachite green assay for released inorganic phosphate.<sup>18</sup>

**Protein Expression and Purification.** SHP-1 and GST-SHP-1(N-SH2) were expressed and purified as previously described.<sup>19</sup> The purity was assessed by SDS–PAGE and determined to be >90%. Dialysis in the experimental buffer was carried out prior to the experiments. In case of the SPR (surface plasmon resonance) measurements, the GST-SHP-1(N-SH2) protein was additionally purified by FPLC (Pharmacia LKB LCC-501 Plus, Pharmacia LKB Biotechnology AB, Uppsala, Sweden) equipped with a Superose 12 column (Amersham Bioscience, Uppsala, Sweden). The protein concentration of GST-SHP-1(N-SH2) for SPR measurements was determined via absorbance at 280 nm using an extinction coefficient of 53.370 M<sup>-1</sup> cm<sup>-1</sup> as calculated from the amino acid sequence<sup>20</sup> and confirmed by quantitative amino acid analysis.

**Phosphatase Activity Assay.** The stimulation of SHP-1 activity was measured using *p*-nitrophenyl phosphate (pNPP) as substrate. The assay reaction (total volume 50 μL) contained 50 mM Hepes, pH 7.4, 50 mM NaCl, 1 mM EDTA, 1 mM tris-(carboxyethyl)phosphine, 10 mM pNPP, 0–500 μM peptide, and 0.5 μg of SHP-1 (100 μg/mL). The reaction was initiated by the addition of SHP-1 as the last component and allowed to proceed at room temperature for 30 min. The reaction was quenched by adding 950 μL of 1 M NaOH. The absorbance was then measured at 405 nm on a Shimadzu BioSpec-1601E. The SHP-1 reactivity reported was relative to that of SHP-1 in the absence of peptide. All measurements were carried out in duplicate, and the results are given as mean value of three independent experiments.

**Surface Plasmon Resonance Analysis.** SPR measurements were carried out on a BIAcore 2000 instrument (Pharmacia Biosensor AB, Uppsala, Sweden). A streptavidin-coated sensorchip (Biacore International SA, Freiburg, Germany) was conditioned with 1 M NaCl/50 mM NaOH according to the manufacturer's instructions. All experiments were carried out at room temperature in Hepes buffer A (10 mM Hepes, 150 mM NaCl, 3.4 mM EDTA, 0.005% surfactant Tween20, pH 7.4). The biotinylated peptides were immobilized onto the sensor chips by flowing a 0.1 μM solution at a flow rate of 10 μL/min until 20–40 response units was reached. A blank flow cell was used as the control for correction of nonspecific binding interactions. Solutions of the GST-SHP-1(N-SH2) protein in Hepes buffer A were injected over the sensorchip for 5 min at a flow rate of 30 μL/min. Dissociation was monitored during subsequent washing of the chip using running buffer A. The chip surface was regenerated after each run using Hepes buffer containing 0.1% SDS (10 s at a flow rate of 30 μL/min). Data analysis was carried out using BIAevaluation 2.0 software. The response of the blank flow cell was subtracted from those of the peptides measured. To avoid sample dispersion effects, a short period after the injection start and stop (10 s) was excluded from the fitting. The equilibrium response units (RU<sub>eq</sub>) were plotted against the concentrations of the N-SH2 domain. To determine the dissociation constant (*K*<sub>d</sub>), the data were fit to the equation  $RU_{eq} = RU_{max}[N-SH2]/(K_d + [N-SH2])$  (RU<sub>eq</sub> is the measured response unit at a given N-SH2 domain concentration, and RU<sub>max</sub> is the maximum response unit).

**Molecular Modeling.** Structural models for the complexes of SHP-1 with various phosphopeptides were generated using the molecular modeling package InsightII (Accelrys Inc., San Diego, CA). The model structures are based on the 2.3 Å crystal structure of the recombinant mouse N-terminal SH2 domain of SHP-2 complexed with the phosphotyrosylpeptide PDGFR-740, with the sequence GGpYMDMS (PDB code 1AYC).<sup>21</sup> The



residues of SHP-2 that are part of the N-SH2 domain binding site and differ from those in SHP-1 were replaced by the corresponding amino acids of SHP-1. According to the sequence alignment of Huyer et al.,<sup>22</sup> the residues V14, K35, S36, K55, K89, E90, and K91 of SHP-2 were replaced by the SHP-1 residues L14, R35, K36, R55, E89, D90, and R91, respectively. Note, that some of the substituted residues contact the pY residue of the bound peptide but none of the substitutions directly contact the residues pY + 1 and pY + 3 of the bound peptide. The complexes were initially modeled using the builder and biopolymer modules of InsightII. Docking into the N-SH2 ligand binding site was performed by exchanging the corresponding residues of the peptide substrate in the experimental complex structure and selection of the best fitting side chain rotamer. The side chains of the substrate in the crystal structure (GGpYMDMS) were replaced by the phosphorylated Ros-derived sequence surrounding pY2267 (EGLNpYMVL) and the synthetic peptides shown in Table 1. The modeled complex conformations were used as starting structures for 800-step conjugated-gradient energy minimization with the protein backbone harmonically restrained to the X-ray coordinates (force constant 100.0 kcal/mol/Å<sup>2</sup>) and free peptides using the cvff-force field as implemented in the discover module of InsightII. An implicit solvent model with a distant dependent dielectric constant of 4.0 was applied. The ranking corresponds to the differences of relative interaction energies between the peptide and the N-terminal SH2 domain relative to the Ros pY2267-SH2 domain interaction (in kcal/mol).

**Acknowledgment.** The authors thank Dr. G. Greiner for amino acid analysis of the peptides and the N-SH2 domain. We are also grateful to Dr. R. Doelling (Biosyntan GmbH, Berlin), and Dr. R. Glaser (Friedrich-Schiller-University, Jena) for valuable discussions. We thank Dr. B. Schlott and A. Wiltzer for excellent technical assistance during SPR measurements and Prof. Dr. F. Grosse for the use of the BIAcore 2000. This work was supported by the Deutsche Forschungsgemeinschaft as part of the collaborative research center SFB 604 (project A1).

## References

- Burke, T. R., Jr.; Zhang, Z. Y. Protein-Tyrosine Phosphatases: Structure, Mechanism, and Inhibitor Discovery. *Biopolymers* **1998**, *47*, 225–241.
- Zhou, Y.; Abagyan, R. How and Why Phosphotyrosine-Containing Peptides Bind to the SH2 and PTB Domains. *Fold. Des.* **1998**, *3*, 513–522.
- Cody, W. L.; Lin, Z.; Panek, R. L.; Rose, D. W.; Rubin, J. R. Progress in the Development of Inhibitors of SH2 Domains. *Curr. Pharm. Des.* **2000**, *6*, 59–98.
- Müller, G. Peptidomimetic SH2 Domain Antagonists for Targeting Signal Transduction. *Top. Curr. Chem.* **2000**, *211*, 17–59.
- Zhang, J.; Somani, A. K.; Siminovitch, K. A. Roles of the SHP-1 Tyrosine Phosphatase in the Negative Regulation of Cell Signaling. *Semin. Immunol.* **2000**, *12*, 361–378.
- Kruger, J.; Butler, J. R.; Cherapanov, V.; Dong, Q.; Ginzberg, H.; Govindarajan, A.; Grinstein, S.; Siminovitch, K. A.; Downey, G. P. Deficiency of Src Homology 2-Containing Phosphatase 1 Results in Abnormalities in Murine Neutrophil Function: Studies in Mice. *J. Immunol.* **2000**, *165*, 5847–5859.
- Umeda, S.; Beamer, W. G.; Takagi, K.; Naito, M.; Hayashi, S.; Yonemitsu, H.; Yi, T.; Shultz, L. D. Deficiency of SHP-1 Protein-Tyrosine Phosphatase Activity Results in Heightened Osteoclast Function and Decreased Bone Density. *Am. J. Pathol.* **1999**, *155*, 223–233.
- Oka, T.; Ouchida, M.; Koyama, M.; Ogama, Y.; Takada, S.; Nakatani, Y.; Tanaka, T.; Yoshino, T.; Hayashi, K.; Ohara, N.; Kondo, E.; Takahashi, K.; Tsuchiyama, J.; Tanimoto, M.; Shimizu, K.; Akagi, T. Gene Silencing of the Tyrosine Phosphatase SHP1 Gene by Aberrant Methylation in Leukemias/Lymphomas. *Cancer Res.* **2002**, *62*, 6390–6394.
- Beghini, A.; Ripamonti, C. B.; Peterlongo, P.; Roversi, G.; Cairoli, R.; Morra, E.; Larizza, L. RNA Hyperediting and Alternative Splicing of Hematopoietic Cell Phosphatase (PTPN6) Gene in Acute Myeloid Leukemia. *Hum. Mol. Genet.* **2000**, *9*, 2297–2304.
- Yip, S. S.; Crew, A. J.; Gee, J. M.; Hui, R.; Blamey, R. W.; Robertson, J. F.; Nicholson, R. I.; Sutherland, R. L.; Daly, R. J. Up-Regulation of the Protein Tyrosine Phosphatase SHP-1 in Human Breast Cancer and Correlation With GRB2 Expression. *Int. J. Cancer* **2000**, *88*, 363–368.
- Yang, J.; Cheng, Z.; Niu, T.; Liang, X.; Zhao, Z. J.; Zhou, G. W. Structural Basis for Substrate Specificity of Protein-Tyrosine Phosphatase SHP-1. *J. Biol. Chem.* **2000**, *275*, 4066–4071.
- Yang, J.; Liu, L.; He, D.; Song, X.; Liang, X.; Zhao, Z. J.; Zhou, G. W. Crystal Structure of Human Protein-Tyrosine Phosphatase SHP-1. *J. Biol. Chem.* **2003**, *278*, 6516–6520.
- Burshtyn, D. N.; Yang, W.; Yi, T.; Long, E. O. A Novel Phosphotyrosine Motif With a Critical Amino Acid at Position -2 for the SH2 Domain-Mediated Activation of the Tyrosine Phosphatase SHP-1. *J. Biol. Chem.* **1997**, *272*, 13066–13072.
- Beebe, K. D.; Wang, P.; Arabaci, G.; Pei, D. Determination of the Binding Specificity of the SH2 Domains of Protein Tyrosine Phosphatase SHP-1 Through the Screening of a Combinatorial Phosphotyrosyl Peptide Library. *Biochemistry* **2000**, *39*, 13251–13260.
- Keilhack, H.; Müller, M.; Böhmer, S. A.; Frank, C.; Weidner, K. M.; Birchmeier, W.; Ligensa, T.; Berndt, A.; Kosmehl, H.; Günther, B.; Müller, T.; Birchmeier, C.; Böhmer, F. D. Negative Regulation of Ros Receptor Tyrosine Kinase Signaling: An Epithelial Function of the SH2 Domain Protein Tyrosine Phosphatase SHP-1. *J. Cell Biol.* **2001**, *152*, 325–334.
- Biskup, C.; Böhmer, A.; Pusch, R.; Kelbauskas, L.; Gorshokov, A.; Majoul, I.; Lindenau, J.; Bendorf, K.; Böhmer, F. D. Visualization of SHP-1 Target Interaction. *J. Cell Sci.* **2004**, *117*, 5165–5178.
- Imhof, D.; Nothmann, D.; Zoda, M. S.; Hampel, K.; Wegert, J.; Böhmer, F. D.; Reissmann, S. Synthesis of Linear and Cyclic Phosphopeptides as Ligands for the Amino-Terminal SH2 Domain of Protein Tyrosine Phosphatase SHP-1. *J. Pept. Sci.* **2004**, in press.
- Harder, K. W.; Owen, P.; Wong, L. K. H.; Aebersold, R.; Clark-Lewis, I.; Jirik, F. R. Characterization and Kinetic Analysis of the Intracellular Domain of Human Protein Tyrosine Phosphatase  $\beta$  (HPTP $\beta$ ) Using Synthetic Phosphopeptides. *Biochem. J.* **1994**, *298*, 395–401.
- Keilhack, H.; Tenev, T.; Nyakatura, E.; Godovac-Zimmermann, J.; Nielsen, L.; Seedorf, K.; Böhmer, F. D. Phosphotyrosine 1173 Mediates Binding of the Protein-Tyrosine Phosphatase SHP-1 to the Epidermal Growth Factor Receptor and Attenuation of Receptor Signaling. *J. Biol. Chem.* **1998**, *273*, 24839–24846.
- Gill, S. C.; von Hippel, P. H. Calculation of Protein Extinction Coefficients from Amino Acid Sequence Data. *Anal. Biochem.* **1989**, *182*, 319–326.
- Lee, H.-E.; Kominos, D.; Jacques, S.; Margolis, B.; Schlessinger, J.; Shoelsen, S. E.; Kuriyan, J. Crystal Structures of Peptide Complexes of the Amino-Terminal SH2 Domain of the Src Tyrosine Phosphatase. *Structure* **1994**, *2*, 423–438.
- Huyer, G.; Ramachandran, C. The Specificity of the N-Terminal SH2 Domain of SHP-2 Is Modified by a Single Point Mutation. *Biochemistry* **1998**, *37*, 2741–2747.
- Arold, H.; Reissmann, S. Synthesis of Bradykinin Analogues Containing threo- $\beta$ -Phenyl Serine. *J. Prakt. Chem.* **1970**, *312*, 1130–1144.
- Arold, H.; Feist, H. Synthesis of Bradykinin Analogues Containing erythro- $\beta$ -Phenyl Serine. *J. Prakt. Chem.* **1970**, *312*, 1145–1160.
- Arold, H.; Reissmann, S.; Eule, M. Synthesis of Bradykinin Analogues Containing  $\alpha$ -Amino- $\beta$ -phenylbutyric Acid. *J. Prakt. Chem.* **1974**, *316*, 93–102.
- Heyl, D. L.; Schmitter, S. J.; Bouzit, H.; Johnson, T. W.; Hepp, A. M.; Kurtz, K. R.; Mousigian, C. Substitution of Aromatic and Nonaromatic Amino Acids for the Phe3 Residue in the Delta-Selective Opioid Peptide Deltorphin I: Effects on Binding Affinity and Selectivity. *Int. J. Pept. Protein Res.* **1994**, *44*, 420–426.
- Hruby, V. J.; Al-Obeidi, F.; Kazmierski, W. Emerging Approaches in the Molecular Design of Receptor-Selective Peptide Ligands: Conformational, Topographical and Dynamic Considerations. *Biochem. J.* **1990**, *268*, 249–262.
- Hruby, V. J. Conformational and Topographical Considerations in the Design of Biologically Active Peptides. *Biopolymers* **1993**, *33*, 1073–1082.
- Hruby, V. J.; Han, G.; Gitsu, P. M. 2003 Synthesis of Side-Chain Conformationally Restricted  $\alpha$ -Amino Acids. In *Houben-Weyl: Methods of Organic Chemistry*, 4th ed.; Goodman, M., Ed.; Georg Thieme Verlag: Stuttgart, 2003; pp 5–51.
- Schiller, P. W.; Weltrowska, G.; Nguyen, T. M. D.; Lemieux, C.; Chung, N. N.; Marsden, B. J.; Wilkes, B. C. Conformational Restriction of the Phenylalanine Residue in a Cyclic Opioid Peptide Analogue: Effects on Receptor Selectivity and Stereospecificity. *J. Med. Chem.* **1991**, *34*, 3125–3132.



(31) Wirth, K.; Hock, F. J.; Albus, U.; Linz, W.; Alpermann, H. G.; Anagnostopoulos, H.; Henke, S.; Breipohl, G.; König, W.; Knolle, J.; Schölkens, B. A. HOE 140 a New Potent and Long Acting Bradykinin-Antagonist: In Vivo Studies. *Br. J. Pharmacol.* **1991**, *102*, 774–777.

(32) Hof, P.; Pluskey, S.; Dhe-Paganon, S.; Eck, M. J.; Shoelson, S. E. Crystal Structure of the Tyrosine Phosphatase SHP-2. *Cell* **1998**, *92*, 441–450.

JM049151T